KINETIC MEAN-FIELD THEORIES

John Karkheck

Department of Mechanical Engineering
State University of New York at Stony Brook
Long Island, New York 11794

and

George Stell

Departments of Chemistry and Mechanical Engineering
State University of New York at Stony Brook
Long Island, New York 11794

Report #350

September 1980

ABSTRACT

A kinetic mean-field theory for the evolution of the one-particle distribution function is derived from maximizing the entropy. For a potential with hard-sphere core plus tail, the resulting theory treats the hard-core part as in the revised Enskog theory. The tail, weighted by the hard-sphere pair distribution function, appears linearly in a mean-field term. The kinetic equation is accompanied by an entropy functional for which an H-theorem was proven earlier. The revised Enskog theory is obtained by setting the potential tail to zero, the Vlasov equation by setting the hard-sphere diameter to zero, and an equation of the Enskog-Vlasov type by effecting the Kac limit on the potential tail. At equilibrium, the theory yields a radial distribution function that is given by that of the hard-sphere reference system and thus furnishes through the internal energy a thermodynamic description which is exact to first order in inverse temperature. A second natural route to thermodynamics (from the momentum flux which yields an approximate equation of state) gives somewhat different results; both routes coincide and become exact in the Kac limit. Our theory furnishes a conceptual basis for the association in the heuristically-based modified Enskog theory (MET) of the contact value of the radial distribution function with the "thermal pressure" since this association follows from our theory (using either route to thermodynamics)

and moreover becomes exact in the Kac limit. Our transport theory is readily extended to the general case of a soft repulsive core, e.g., as exhibited by the Lennard-Jones potential, via by-now-standard statistical-mechanical methods involving an effective hard-core potential, thus providing a self-contained statistical-mechanical basis for application to such potentials that is lacking in the standard versions of the MET. We obtain very good agreement with experiment for the thermal conductivity and shear viscosity of several saturated simple liquids.

1. INTRODUCTION

A number of approaches have been taken for the development of microscopic theories of transport in liquids. Notable among the kinetic-equation approaches are those of Kirkwood and co-workers,[1] Born and Green,[2] Rice-Allnatt,[3] and Davis, Rice and Sengers.[4] In addition, there is the Green-Kubo formalism[5] which relates linear transport coefficients to integrals of time-correlation functions. All of these approaches have produced transport theories which tend to be technically complicated when applied to the liquid state. As yet they have had only limited success in producing expressions for transport coefficients that are both analytically tractable and satisfactorily accurate. Furthermore, the kinetic theories do not appear to have been provided with entropy functionals and H-theorems which characterize the irreversibility and approach to equilibrium of kinetic equations.[6] In contrast, the kinetic theory for the dense hard-sphere fluid introduced and developed by Enskog,[7a] (SET),[7b] and recently improved by van Beijeren and Ernst[8] in order to satisfy the Onsager reciprocal relations, is both analytically tractable and relatively accurate. Moreover, this revised Enskog theory (RET) has been shown by Resibois[9] to include an entropy functional and to have an H-theorem. This theory clearly deserves to be extended to more realistic potentials. Such an extension is given here.

Several routes[7a,10] have already been developed for the purpose of relating the transport coefficient formulae of Enskog theory and its multicomponent generalizations[8,11] to real fluids. The difficulties in

applying the SET and RET transport coefficient formulae lie in relating the contact values of the hard-sphere radial distribution functions (rdf) and the hard-sphere diameters that appear in the theory, to quantities associated with real liquid systems (or even with realistic model systems such as Lennard-Jones systems). Enskog suggested[7a] the interpretation of the contact value of the rdf not in terms of the hard-sphere model but rather in terms of the "thermal pressure" of the fluid. Approaches based upon this association (which is only clear-cut in the one-component case) have come to be known as the modified Enskog theory (MET).[10a] (Variants can be found in the determination of the hard-sphere diameter.[12]) Although useful in the dense gas regime,[7a] the MET has met with only moderate success in application to saturated liquids.[10a]

We describe here the properties of a kinetic mean-field theory and apply it to a description of the transport properties of saturated simple liquids. Its simplest version is a kinetic variational theory based upon the maximization of entropy. Details of the derivation of the resulting kinetic equation and entropy functional, and demonstration of an H-theorem, are given elsewhere.[13] A potential with a hard-sphere core plus an attractive tail is assumed. The hard-core part is treated as it is in the RET to produce the collision term which is the source of irreversibility. The tail, on the other hand, enters the kinetic equation only linearly, in a mean-field type term. This mean-field term contributes to the momentum flux in such a way that at equilibrium we obtain the formula for fluid pressure that comes from approximating the full radial distribution function by that of the hard-sphere reference system. An analogous

result is obtained for the equilibrium internal energy. As a consequence, the equilibrium internal energy (and derived entropy and free energy functions) are all found to be exact through first order in potential tail strength and in inverse temperature.

A number of previous results in kinetic theory follow as limits of our kinetic variational equation. The RET is recovered by setting the attractive tail to zero, the Vlasov equation by setting the hard-sphere diameter to zero, and an Enskog-Vlasov type equation[14] by taking the Kac limit[15] on the attractive tail. The theory plays a role in kinetic theory analogous to that of the mean-spherical approximation of equilibrium statistical mechanics[16] which yields the Percus-Yevick approximation when the tail is set to zero, the Debye-Hückel approximation when the hard-sphere diameter is set to zero, and a van der Waals-like approximation in the Kac limit. Viewed in this context, the RET is conceptually analogous to the Percus-Yevick approximation.

The thermal conductivity and viscosities which follow from our kinetic variational equation are identical functions of temperature and density to those of the RET. Thus, in application to these transport phenomena, the kinetic variational theory enjoys the mathematical tractability of the Enskog theory. Moreover, it provides a theoretical basis for the MET, which associates the contact value of the rdf (for a one component fluid) with the thermal pressure. This association is a precise consequence of the systematic development of our theory for a hard-core potential with arbitrary tail strength. Effecting the Kac limit upon the tail makes this association exact.

Our theory naturally leads toward use of the statistical mechanical procedures[17-20] that have become standard in equilibrium theory to select a state-dependent hard-sphere reference potential in relation to a full potential, e.g. of Lennard-Jones type. Thus we have available to us a means of treating a much wider class of potentials. That is, we have at hand several prescriptions for the application of the hard-sphere model, in terms of hard-sphere quantities, to a description of the transport properties of simple liquids whose equilibrium properties are well-represented by the same hard-sphere reference system.

The kinetic variational theory just described has a fundamental limitation--it treats the contribution to transport coefficients coming from the repulsive core of the pair interaction on the level of accuracy of the hard-sphere RET, and the hard-sphere RET is known to be in significant quantitative error in its assessment of self-diffusion and, to a lesser extent, shear viscosity at the high densities that typify the liquid state. We therefore go on to generalize the kinetic variational theory to a kinetic mean-field theory in which the effect of the attractive tail part of the pair interaction is handled just as before, but the effect of the hard core is treated exactly, in principle. We shall call this our kinetic reference theory (KRT). The kinetic equation associated with this theory can no longer be analyzed as before to yield explicit transport coefficient formulae. However, through numerical simulation[21] the transport properties of the hard-sphere reference system are already known. With this basis, it is easily shown that the transport coefficients of the kinetic reference theory are identical functions of density and

temperature as the exact hard-sphere quantities, for which an adequate description has been given by molecular dynamics simulation.[21] It is well known that these MD quantities may be expressed in terms of the RET expressions which are appended with suitable correction factors.[22]

We compare both corrected and uncorrected RET transport-coefficient predictions to experimental data for several simple liquids along the liquid-vapor saturation curve, using the results of the Weeks-Chandler-Anderson,[17] Mansoori-Canfield[18]/Rasaiah-Stell,[19] and Barker-Henderson[20] prescriptions to obtain a hard-sphere diameter that is state-dependent and depends also on the chosen Lennard-Jones parameters. We obtain good overall agreement. Moreover, for each transport coefficient at least one of the procedures for obtaining the effective hard-sphere diameter yields results of remarkable quantitative accuracy, and we begin in this paper to investigate the question of which of the prescriptions is most appropriate for the computation of each transport coefficient for real fluids. We find in addition that excellent agreement with MD simulated shear viscosity can be had by insertion of WCA[17] diameters into the corrected-Enskog shear viscosity formula.

In section 2 we introduce the kinetic variational theory, construct the hydrodynamic equations and identify the fluxes of mass, heat and momentum, which contains the pressure tensor. In section 3, we describe the thermodynamics associated with the theory and demonstrate how the variational theory justifies the MET procedure from first principles. In section 4 we generalize to the kinetic reference theory and in section 5, we apply the approximations we have developed to prediction of the thermal conductivities and shear viscosities of saturated liquid argon, xenon and oxygen, and also compare theory to MD simulation results. We close with a discussion in section 6.

II. KINETIC VARIATIONAL THEORY, HYDRODYNAMIC EQUATIONS, AND FLUXES

For a single-species fluid with a pair potential of the form

$$\begin{aligned} \phi(r) &= \infty, \qquad r < \sigma \\ &= \phi_t(r), \quad r > \sigma \end{aligned} \tag{1}$$

the dynamic equation for the one-particle generic distribution function $f_1(x_1,t)$ can be written as[13]

$$\left(\frac{\partial}{\partial t} + \vec{v}_1 \cdot \nabla_1\right) f_1(x_1,t) = \frac{1}{m} \frac{\partial}{\partial \vec{v}_1} f_1(x_1,t) \cdot \int dx_2 \, \hat{r}_{12} \phi_t'(r_{12}) f_1(x_2,t) G(x_1,x_2,t)$$
$$+ \sigma^2 \int d\vec{v}_2 \int d\hat{\sigma} \, \hat{\sigma} \cdot \vec{g} \theta(\hat{\sigma} \cdot \vec{g}) \Big\{ G(\vec{r}_1, \vec{v}_1', \vec{r}_1 + \sigma\hat{\sigma}, \vec{v}_2', t) f_1(\vec{r}_1, \vec{v}_1', t) f_1(\vec{r}_1 + \sigma\hat{\sigma}, \vec{v}_2', t)$$
$$- G(\vec{r}_1, \vec{v}_1, \vec{r}_1 - \sigma\hat{\sigma}, v_2, t) f_1(\vec{r}_1, \vec{v}_1, t) f_1(\vec{r}_1 - \sigma\hat{\sigma}, \vec{v}_2, t) \Big\}, \tag{2}$$

In (2), x_i is the vector $(\vec{r}_i, \vec{v}_i)$, m is particle mass, $\vec{g} = \vec{v}_2 - \vec{v}_1$, $\phi_t'(r_{12})$ is $d\phi_t(r_{12})/dr_{12}$, $\hat{r}_{12}$ is the unit vector $\vec{r}_{12}/|\vec{r}_{12}|$, θ is the Heaviside function and $G(x_1,x_2,t)$ is defined as the ratio of the generic two-particle distribution function to the product of two one-particle functions,

$$f_2(x_1,x_2,t)/f_1(x_1,t)f_1(x_2,t) = G(x_1,x_2,t). \tag{3}$$

In (2) and throughout this article, we display the arguments of functions like f_1, f_2, G, etc. in terms of either the x_i or the individual $\vec{r}_i$ and $\vec{v}_i$, depending upon the dictates of the particular expressions in which they appear. The local number density, average velocity, and temperature are defined by

$$n(\vec{r}_1,t) = \int d\vec{v}_1 f_1(x_1,t) \tag{4a}$$

$$n\vec{u}(\vec{r}_1,t) = \int d\vec{v}_1 \vec{v}_1 f_1(x_1,t) \tag{4b}$$

$$\tfrac{3}{2} nkT(\vec{r}_1,t) = \int d\vec{v}_1 \tfrac{1}{2} m(\vec{v}_1 - \vec{u})^2 f_1(x_1,t). \tag{4c}$$

Equation (2) is exact, but $G(x_1,x_2,t)$ is unknown in general. The equation that we shall call the kinetic variational equation for f_1 follows from using in (2) the approximation

$$G(x_1,x_2,t) = g_2^{HS}(\vec{r}_1,\vec{r}_2|n) \tag{5}$$

where $g_2^{HS}(\vec{r}_1,\vec{r}_2|n)$ is the form assumed by G for a hard-sphere system (i.e. for $\phi_t \equiv 0$) in inhomogeneous equilibrium with number density $n(\vec{r},t)$. The equation for f_1 that results is implied by the maximization of entropy subject to certain constraints appropriate to the potential form given by (1), as we have shown elsewhere.[13] It is for this reason that we refer to the resulting theory as a kinetic-variational (KV) theory. We shall now briefly summarize some of its implications.

Throughout the following development G is given by (5). Applying (4a) to (2), we obtain the continuity equation

$$\frac{\partial}{\partial t} n(\vec{r}_1,t) + \nabla_1 \cdot n\vec{u}(\vec{r}_1,t) = 0, \tag{6a}$$

and applying (4b) to (2) we get the intermediate result, where

$$\overleftrightarrow{P^s} = \int d\vec{v}_1 m(\vec{v}_1-\vec{u})(\vec{v}_1-\vec{u}) f_1(\vec{r}_1,\vec{v}_1,t),$$

$$\frac{\partial}{\partial t} n\vec{u} + \nabla_1 \cdot \left(\frac{1}{m}\overleftrightarrow{P^s} + n\vec{u}\,\vec{u}\right) = -\frac{1}{m}\int d\vec{r}_3 d\vec{r}_2 \hat{r}_{32}\phi_t'(r_{32}) n_2^{HS}(\vec{r}_3,\vec{r}_2|n)\delta(\vec{r}_3-\vec{r}_1)$$

$$+ \sigma^2 \int d\vec{v}_1 d\vec{v}_2 \int d\hat{\sigma}\ \hat{\sigma}\cdot\vec{g}\theta(\hat{\sigma}\cdot\vec{g})(\vec{v}_1'-\vec{v}_1) g_2^{HS}(\vec{r}_1,\vec{r}_1-\sigma\hat{\sigma}|n)$$

$$\cdot f_1(\vec{r}_1,\vec{v}_1,t) f_1(\vec{r}_1-\sigma\hat{\sigma},\vec{v}_2,t). \tag{6b}$$

Here $n_2^{HS}(\vec{r}_3,\vec{r}_2|n) = n(\vec{r}_3,t)n(\vec{r}_2,t)g_2^{HS}(\vec{r}_3,\vec{r}_2|n) = n_2^{HS}(\vec{r}_2,\vec{r}_3|n)$. Symmetrization of the first term on the RHS of (6b) yields

$$-\frac{1}{2m}\int d\vec{r}_3 d\vec{r}_2 \hat{r}_{32} n_2^{HS}(\vec{r}_3,\vec{r}_2|n)[\delta(\vec{r}_3-\vec{r}_1)-\delta(\vec{r}_2-\vec{r}_1)]\phi_t'(r_{32})$$

$$=\frac{1}{2m}\nabla_1\cdot\int d\vec{r}_3 d\vec{r}_2 \vec{r}_{32}\hat{r}_{32} n_2^{HS}(\vec{r}_3,\vec{r}_2|n)\phi_t'(r_{32})\int_0^1 d\lambda\ \delta[\lambda(\vec{r}_3-\vec{r}_2)+\vec{r}_2-\vec{r}_1]$$

$$=\frac{1}{2m}\nabla_1\cdot\int_0^1 d\lambda\int ds\, \vec{s}\hat{s}\, n_2^{HS}(\vec{r}_1+\lambda\vec{s}-\vec{s},\vec{r}_1+\lambda\vec{s}|n)\phi_t'(s)$$

$$\equiv -\frac{1}{m}\nabla_1\cdot\overleftrightarrow{P}^t. \tag{6c}$$

The superscript s denotes a streaming contribution while t denotes a contribution arising from the presence of the tail term.

Symmetrization of the second term on the RHS of (6b) yields, where $f_2 = g_2^{HS} f_1 f_1$ is to be understood,

$$-\frac{1}{2}\sigma^3\nabla_1\cdot\int d\vec{v}_1 d\vec{v}_2\int d\hat{\sigma}\,\hat{\sigma}\,\hat{\sigma}\cdot\vec{g}\,\theta(\hat{\sigma}\cdot\vec{g})(\vec{v}_1'-\vec{v}_1)\int_0^1 d\lambda f_2(\vec{r}_1+\lambda\sigma\hat{\sigma},\vec{v}_1,\vec{r}_1+\lambda\sigma\hat{\sigma}-\sigma\hat{\sigma},\vec{v}_2,t)$$

$$\equiv -\frac{1}{m}\nabla_1\cdot\overleftrightarrow{P}^c. \tag{6d}$$

The superscript c here denotes a contribution arising from the hard-core collision. Eliminate $\frac{\partial}{\partial t}n$ from (6b) using (6a) to obtain the equation of motion:

$$n\left(\frac{\partial}{\partial t}+\vec{u}\cdot\nabla\right)\vec{u}(\vec{r}_1,t)+\frac{1}{m}\nabla\cdot(\overleftrightarrow{P}^s+\overleftrightarrow{P}^t+\overleftrightarrow{P}^c)=0. \tag{7}$$

Apply (4c) to (2) to obtain the intermediate result

$$\frac{\partial}{\partial t}\left(\frac{3}{2}nkT+\frac{1}{2}nmu^2\right)+\nabla_1\cdot\left(\vec{J}_T^{s+c}+\frac{3}{2}nkT\vec{u}+\overleftrightarrow{P}^{s+c}\cdot\vec{u}+\frac{1}{2}nmu^2\vec{u}\right.$$

$$\left.+\vec{u}\cdot(\nabla_1\cdot\overleftrightarrow{P}^t)\right)=0,$$

which simplifies, when $\frac{\partial}{\partial t}n$, $\frac{\partial}{\partial t}\vec{u}$ are eliminated via (6a) and (7), to:

$$n\left(\frac{\partial}{\partial t}+\vec{u}\cdot\nabla_1\right)\frac{3}{2}kT+\nabla_1\cdot\vec{J}_T^{s+c}+\overleftrightarrow{P}^{s+c}:\nabla_1\vec{u}=0 \tag{8}$$

which is the temperature equation. The streaming and collisional

heat fluxes are:

$$\vec{J}_T^{\,s} = \int d\vec{v}_1 \frac{1}{2} m(\vec{v}_1-\vec{u})^2(\vec{v}_1-\vec{u}) f_1 \tag{9a}$$

$$\vec{J}_T^{\,c} = \frac{1}{2} m\sigma^3 \int d\vec{v}_1 d\vec{v}_2 \int d\hat{\sigma}\hat{\sigma}\cdot\vec{g}\theta(\hat{\sigma}\cdot\vec{g})(\vec{v}_1'-\vec{v}_1)\cdot\left(\frac{\vec{v}_1'+\vec{v}_1}{2} - \vec{u}\right)$$

$$\times \int_0^1 d\lambda f_2(\vec{r}_1+\lambda\sigma\hat{\sigma},\vec{v}_1,\vec{r}_1+\lambda\sigma\hat{\sigma}-\sigma\hat{\sigma},\vec{v}_2,t). \tag{9b}$$

Note that the potential enters the momentum flux, $\overleftrightarrow{P} = \overleftrightarrow{P}^s + \overleftrightarrow{P}^c + \overleftrightarrow{P}^t$, but not the temperature-heat fluxes. The potential energy density at $(\vec{r},t)$ is given in general by:

$$u_p(\vec{r},t) = \frac{1}{2}\int dx_1 dx_2 f_2(x_1,x_2,t)\phi(r_{12})\delta(\vec{r}_1-\vec{r}) \tag{10a}$$

and in our case $f_2 = g_2^{HS} f_1 f_1$ yields

$$u_p(\vec{r},t) = \frac{1}{2}\int d\vec{r}_1 d\vec{r}_2 n_2^{HS}(\vec{r}_1,\vec{r}_2|n)\phi(r_{12})\delta(\vec{r}_1-\vec{r}) \tag{10b}$$

hence $\frac{\partial u_p}{\partial t}$ depends only upon $\frac{\partial n}{\partial t}$ which does not couple to inhomogeneities in the temperature field in the one component, linear, case. Thus there is no contribution from the potential tail to the heat flux.[23] In summary, we obtain heat and mass fluxes identical in form and content to those found in the revised Enskog theory[8] by following the procedure used in ref. 24. There is an additional term in the momentum flux, above and beyond that of revised Enskog theory, which arises from the tail part of the potential. Furthermore, the tail does no work on the system [cf. (8)] and this result is compatible with the observation that the mean-field term does not contribute to entropy production.[13] Hence, as direct calculation bears out, we can infer that the thermal conductivity, bulk and shear viscosities that may be obtained from (2) with (5) via the Chapman-Enskog

development[25] are identical functions of T and n to those of the SET (which yields the same three transport coefficients, for a one-component fluid, as the RET). Thus, with respect to these properties, the only (but hardly trivial) distinction between our kinetic variational theory, (2) and (5), and the Enskog theory[7a] lies in the momentum flux, specifically in the tail contribution found in the former.

III. THERMODYNAMICS OF THE KINETIC VARIATIONAL THEORY

As we have proved elsewhere,[13] there is an H-theorem associated with the KVT. At equilibrium, equation (3) relaxes into the relation $f_2^{eq} = g_2^{HSeq} f_1^{eq} f_1^{eq}$, whereby we obtain for P^s and P^c the well-known results embedded in the SET[7a]

$$P^s = nkT \tag{11a}$$

$$P^c = \frac{2}{3}\pi\sigma^3 n^2 kT\, y_2(\sigma;n) \tag{11b}$$

where $y_2(\sigma;n)$ is the contact value of the hard-sphere rdf. In addition we find, from (6c),

$$P^t = -\frac{2\pi}{3} n^2 \int_\sigma^\infty dr\, r^3 \phi_t'(r) g_2^{HSeq}(r;n)\ , \tag{11c}$$

and the full pressure is given by $P = P^s + P^c + P^t$. We also find the energy per particle, e,

$$e = e_k + e_p \tag{12a}$$

where

$$e_k = \frac{3}{2}kT \tag{12b}$$

and, from (10b)

$$e_p = \frac{u_p}{n} = 2\pi n \int_\sigma^\infty dr\, r^2 \phi_t(r) g_2^{HSeq}(r;n). \tag{12c}$$

Hence the theory provides two distinct thermodynamic descriptions. Using (12) and

$$e = \frac{\partial}{\partial\beta}(\beta f)_n \tag{13}$$

we obtain the free-energy per particle, f_e, originating from energy:

$$f_e = f^{HS} + 2\pi n \int_\sigma^\infty dr\, r^2 \phi_t(r) g_2^{HSeq}(r;n). \tag{14}$$

Alternately, using (11) and

$$P = n^2\left(\frac{\partial f}{\partial n}\right)_T \tag{15}$$

we obtain the free-energy per particle, f_p:

$$f_p = f^{HS} - \frac{2\pi}{3}\int_0^n dn' \int_\sigma^\infty dr\ r^3\phi_t'(r)g_2^{HSeq}(r;n'). \tag{16}$$

In general, $f_p \neq f_e$. Both (14) and (16) contain the same exact hard-sphere reference free energy f^{HS}, however (14) also contains all contributions to the exact f through order $(kT)^0$, as found in perturbation theory,[26,27] whereas (16) is lacking a term of this order. Hence, the thermodynamic descriptions, based upon (14) and (16) will, in general, be different. We now distinguish three cases.

(A) The Kac-tail Limit

Upon introducing the Kac potential[15]

$$\phi_t(r) = \lim_{\gamma\to 0} \gamma^3 V(\gamma r) \tag{17}$$

into (11c) we obtain the well-known result

$$P^t = -an^2 \tag{18}$$

where $a = -2\pi\int_0^\infty dx\ x^2V(x)$ is a constant. Also, one obtains $f_p = f_e = f$ where f is the exact result as obtained, e.g. from the partition function. Hence, in this limit, (17), the kinetic-variational theory embodies the exact thermodynamic description for a potential consisting of hard-sphere core and an infinitely weak long-range attraction. In particular, we find that the tail does not change the entropy of the system, i.e.

$$s = -\left(\frac{\partial f}{\partial T}\right)_n = s^{HS}.$$

The entropy obtained from f [either (14) or (16) in the limit (17)] is precisely the same function which the nonequilibrium entropy functional that accompanies the kinetic variational equation[13] relaxes to in equilibrium.

In the limit (17), the mean-field term in (2) with (5) takes the form of a Vlasov mean-field term and the full kinetic equation takes the form of an Enskog-Vlasov type equation.[13,14] The full pressure is given by [cf. (11)]:

$$P = nkT[1 + \tfrac{2}{3}\pi\sigma^3 n\, y_2(\sigma;n)] - an^2. \qquad (19)$$

As already noted, the transport coefficients for this theory are the same functions of T and n as those of Enskog theory,[7a] in which y_2 plays a fundamental role. Enskog used the equation of state, (19), as a means to relate the hard sphere transport coefficients to experimental quantities.[28a] The ingredients for a second approach,[28b] based upon the association

$$\frac{2}{3}\pi n\sigma^3\, y_2(\sigma;n) = \frac{T\left(\frac{\partial P}{\partial T}\right)_V - nkT}{nkT}, \qquad (20)$$

where $T\left(\frac{\partial P}{\partial T}\right)_V$ is the "thermal pressure" of the fluid under study, are contained in Enskog's paper.[7a] Upon differentiation with respect to T, an identical expression follows rigorously from (19), which we now know to be a good qualitative representation of the real-fluid equation of state.

Furthermore, in the limit (17), the tail contributions to the transport coefficients obtained via more rigorous theory[29] vanish, so that the hard-sphere forms (for which Enskog theory gives an approximate representation) represent the full contributions to the transport coefficients.

(B) KVT with Arbitrary Soft Tail

In this case, the tail (assumed to have no discontinuity except at $r = \sigma$) can take any form, but the hard-sphere diameter is fixed. Then P^t, (11c), and e_p, (12c), are still temperature independent. Thus (14) and (16) yield the same entropy, s^{HS}, as before (case A) and in agreement with the kinetic-theoretic quantity,[13] evaluated at equilibrium. That is, the tail again does not change s from the hard-sphere reference value.[27] Though the thermodynamic descriptions derived from (14) and (16) disagree, both free energies again lead to the association (20); despite disagreement between tail contributions to the pressure, both contributions are temperature independent. Hence the KVT supports the association (20) in a broader context than just the van der Waalsian equation of state (19) which was the original basis for (20).[7a] We note that the thermodynamics obtained from (16) is inferior to that from (14); for example, the equation of state (11) is not as accurate as that which follows from (14). Furthermore, because (14) is exact to first order in perturbation expansion, the Gibbs-Bogoliubov inequality renders[27]

$$f \leq f_e \tag{21}$$

where f is the exact free energy.

(C) The KVT with Optimized Thermodynamics

The hard-sphere diameter, σ, may be made state dependent by choosing it to minimize the upper bound f_e in (21), as was done by

MC[18]/RS[19], or to optimally mimic a smooth-potential fluid, treated approximately, in other ways.[17,20] This optimization is made on equilibrium properties. We take up this last case again in section 5 where the $\sigma(T,n)$ are used in a study of transport properties of simple fluids.

IV. KINETIC REFERENCE THEORY

A number of generalizations of the KVT may be contemplated. Here we consider one of them. Computer simulations[21] have demonstrated large deficiencies in the RET shear viscosity and self-diffusion coefficients at densities characteristic of the liquid state. It is clear that the same deficiencies are present in the KVT transport coefficients for the more general class of potentials treated by the theory.

Quantitative improvement upon the KVT in this regard can be had by replacing the variation-based approximation (5) with the quantity

$$G(x_1,x_2,t) = G^{HS}(x_1,x_2,t) \tag{22}$$

in the collision term of (2), where the G^{HS} is the exact two-particle correlation function for the hard-sphere fluid. We call the theory generated by this new equation

$$\left(\frac{\partial}{\partial t}+\vec{v}_1\cdot\nabla_1\right)f_1(x_1,t) = \frac{1}{m}\frac{\partial}{\partial\vec{v}_1}f_1(x_1,t)\cdot\int d\vec{r}_2\hat{r}_{12}\phi_t'(r_{12})n(\vec{r}_2,t)g_2^{HS}(\vec{r}_1,\vec{r}_2|n)$$
$$+\sigma^2\int d\vec{v}_2\int d\hat{\sigma}\;\hat{\sigma}\cdot\vec{g}\theta(\hat{\sigma}\cdot\vec{g})\{G^{HS}(\vec{r}_1,\vec{v}_1',\vec{r}_1+\sigma\hat{\sigma},\vec{v}_2',t)f_1(\vec{r}_1,\vec{v}_1',t)f_1(\vec{r}_1+\sigma\hat{\sigma},\vec{v}_2',t)$$
$$-G^{HS}(x_1,\vec{r}_1-\sigma\hat{\sigma},\vec{v}_2,t)f_1(x_1,t)f_1(\vec{r}_1-\sigma\hat{\sigma},\vec{v}_2,t)\} \tag{23}$$

the kinetic reference theory (KRT).

The G^{HS} is unknown in form; therefore (23) is not solvable to produce explicit transport coefficient formulae. However, the fluxes and hydrodynamic equations may be constructed. It is found that the mean-field term enters these in KRT in the same way as for KVT. Thus the potential tail does not enter the transport coefficient formulae explicitly, and the thermodynamics embedded in KRT is the

same as for KVT, since G^{HS} relaxes to g_2^{HSeq} at equilibrium. Furthermore, though we cannot obtain explicit transport coefficient formulae from (23), the transport coefficients of the KRT are the exact hard-sphere transport coefficients for which a description has been obtained via molecular dynamics[21] (MD) from which in turn analytic expressions have been developed[22] in the form of density dependent multiplicative correction factors appended to the transport coefficient formulae of the SET.

V. APPLICATIONS

We shall now explicitly consider the question of how to interpret and determine the σ and y_2 appearing in our formulae [e.g., Eqs. (27)] when applying them to real fluids, contrasting our method with that of the MET.

The MET interpretation typically has three ingredients.[10a,28] The association (20) provides two of these. First, the real-fluid thermal pressure is inserted into the RHS of (20). To disentangle σ^3 and y_2, the low density limit, $n \to 0$ (in which $y_2 = 1$) is used, thereby associating σ^3 with the real-fluid second virial coefficient and its temperature derivative. Finally, the λ_o and η_o appearing in (27a,b) [which take the explicit forms (27c,d) in the SET] are interpreted as the dilute-gas transport coefficients for the real substance under consideration. The MET transport coefficients defined in this way yield correct transport properties in the low-density limit by construction. We note, however, that the assurance of an internally consistent effective hard-sphere diameter of the fluid has been lost through this combination of procedures. The problem is that the σ defined by (20) is both density and temperature dependent, while the σ defined by the low-density limit of that expression is only temperature dependent. Moreover, its temperature dependence is not in general the same as that given by Eq. (27c,d) when either real-gas or model (e.g., Lennard-Jones) values for λ_o and η_o are taken.

The interpretation that we have utilized here in our applications of the formulae (27) instead maintains a hard-sphere fluid representation of the real fluid by consistently employing the same state-dependent σ throughout (27) and (28). In fact, by using any of the three well-known approaches[17-20] available for assigning this σ, we automatically achieve a consistent portrayal of the real-fluid equilibrium and transport properties through a single equivalent-hard-sphere-fluid representation. This state-dependent diameter approach, described in detail below, is conceptually and technically different than the MET. Conceptually, the most striking advantage our model has over the MET is that it does not rely on supplementary thermodynamic (PVT and second virial coefficient) input, nor on dilute-gas transport properties, both of which are essential ingredients in the MET. We apply below the state-dependent-diameter approach to a description of the thermal conductivity and shear viscosity of simple liquids which are described by the Lennard-Jones 6-12 potential. Hence, as input we require atomic masses, LJ parameter values, and only the temperature and density of the state point. As we shall see, the results compare favorably to those transport quantities experimentally determined for argon, xenon and oxygen.

We model the Lennard-Jones potential

$$\phi(r) = 4\varepsilon\left[\left(\frac{\sigma_{LJ}}{r}\right)^{12} - \left(\frac{\sigma_{LJ}}{r}\right)^{6}\right] \tag{24}$$

which we assume to be a good representation of the inter-particle potential for real simple liquids. A number of ways have been proposed[17-20] to approximate the equilibrium properties of a liquid described by the potential (24) through an optimally chosen hard-sphere reference potential and a perturbing potential which is treated in first order perturbation theory. We will not go into detail on these techniques, but only summarize here the salient results. Barker and Henderson[20] (BH) focus on a piece of the repulsive part of the potential (24) to obtain a hard-sphere diameter that is temperature dependent and is closely approximated by the formula[17b]

$$\sigma^{BH} = \sigma_{LJ}\,\frac{1.068 + 0.3837\frac{kT}{\varepsilon}}{1 + 0.4293\frac{kT}{\varepsilon}}\,. \tag{25}$$

Weeks, Chandler and Anderson[17a] (WCA) consider the whole repulsive part of the potential and obtain a hard-sphere diameter that is temperature and density dependent. As shown by Verlet and Weis ,[17b]

a good approximation for the WCA diameter is given by the expression

$$\sigma^{WCA} = \sigma^{BH}\left(1 + \frac{A}{B}\right) \tag{26}$$

where

$$A = \frac{1 - 4.25\ Y_w + 1.362\ Y_w^2 - 0.8751\ Y_w^3}{(1 - Y_w)^2}$$

$$B = 210.31 + 404.6\ \frac{\varepsilon}{kT}$$

$$Y_w = Y - \frac{1}{16}\ Y^2$$

$$Y = \frac{\pi}{6} n\ (\sigma^{WCA})^3.$$

As already mentioned, Mansoori and Canfield[18] (MC) and Rasaiah and Stell[19] (RS) find the least upper bound to f [cf. (21)], i.e. minimize f_e, (14), hence making σ both temperature and density dependent.

(A) Comparison of Theory and Experiment

In the applications that follow we begin to assess which of the three approaches to diameter assignment renders the most accurate predictions of the transport properties of real simple liquids and also what L-J parameter values are appropriate. The experimental data for transport properties and saturation lines used in this connection was obtained from ref. 30.

Inasmuch as the models we use satisfy the conditions for applicability of the principle of corresponding states,[31] the theoretical transport properties of the model fluids will appear similar. It appears that the noble liquids conform quite closely[32] to a simple corresponding-states principle,[31] and indeed this feature has been exploited in ref. 30 to generate the transport properties of xenon and krypton from those of argon. However, it appears that liquid oxygen conforms more closely to a generalized corresponding-states

principle which accommodates rotational degrees of freedom.[33] These qualitative differences manifest themselves in our results, as will be seen.

The remaining ingredients that have gone into our comparison of theory and experiment are:

1. The Enskog expressions:[7a]

thermal conductivity λ

$$\frac{\lambda}{\lambda_o} = \frac{1}{y_2}\left[1 + \tfrac{4}{5}\pi n\sigma^3 y_2 + 0.757\left(\tfrac{2}{3}\pi n\sigma^3 y_2\right)^2\right] \tag{27a}$$

shear viscosity η_E

$$\frac{\eta_E}{\eta_o} = \frac{1}{y_2}\left[1 + \tfrac{8}{15}\pi n\sigma^3 y_2 + 0.761\left(\tfrac{2}{3}\pi n\sigma^3 y_2\right)^2\right] \tag{27b}$$

and dilute hard-sphere gas values:

$$\lambda_o = \tfrac{43}{42} \cdot \tfrac{75}{64}\, k\, \sqrt{k/\pi m}\, \frac{T^{1/2}}{\sigma^2} \tag{27c}$$

$$\eta_o = 1.016\, \tfrac{5}{16}\, \sqrt{mk/\pi}\, \frac{T^{1/2}}{\sigma^2}. \tag{27d}$$

2. Numerical corrections[22] to η_E via molecular dynamics simulations.[21] These corrections characterize the deficiency of KVT hard-sphere shear viscosity, and when applied to (27b) yield the KRT shear viscosity, η, which is conceptually exact for the hard-sphere fluid.

3. The Carnahan-Starling expression[34] for y_2:

$$y_2 = \frac{1 - \frac{\pi}{12} n\sigma^3}{\left(1 - \frac{\pi}{6} n\sigma^3\right)^3}. \tag{28}$$

4. For σ we use the BH diameters obtained from (25), or the WCA diameters obtained from (26), or the MC/RS diameters obtained by minimizing (14), using an analytic approximation for the integral in (14) which follows from the results of Larsen et al.[35]

We note that for all but one experimental point (T = 150K for argon) we observe that

$$\sigma^{MC/RS}(T,n) < \sigma^{WCA}(T,n) \lesssim \sigma^{BH}(T) \tag{29}$$

which implies that

$$\lambda^{MC/RS}(T,n) < \lambda^{WCA}(T,n) \lesssim \lambda^{BH}(T) \tag{30}$$

and similarly for shear viscosity, η_E, and its MD corrected counterpart, η.

In figures 1 and 2 are shown various predictions of theory for ε/k = 119.8K and σ_{LJ} = 3.405 Å. This L-J set has been used extensively for relating equilibrium theory to the properties of argon, and, clearly, yields very good agreement with experiment for both transport coefficients, with judicious choice of calculational route. First we note that the KVT and KRT are superior to the DRS[36] theory in this application. We observe that $\sigma^{MC/RS}$ yields a good theoretical λ but a relatively poor η_E and η. Indeed, no amount of adjusting ε and σ_{LJ} can force $\eta_E^{MC/RS}$ or $\eta^{MC/RS}$ up without at the same time raising $\lambda^{MC/RS}$. Thus the MC/RS approach exclusively is not the route for best fit of both transport coefficients. The combinations λ^{BH} and η^{BH}, or λ^{WCA} and η^{WCA}, can yield a closer fit (by adjustment of ε and σ_{LJ}) than shown here, however. The need for MD corrections on shear viscosity, i.e., the superiority of KRT to KVT, is apparent here, especially so at the lower temperatures and higher densities. Save that visual comparison suggests the overall best fit is to be had with the combination $\lambda^{MC/RS}$ and either η^{WCA} or η^{BH}, we cannot conclude from this figure whether a single thermodynamic optimization or a combination of approaches is best.

That a combination of approaches, e.g. $\lambda^{MC/RS}$ and η^{WCA} or $\lambda^{MC/RS}$ and η^{BH}, seems necessary for overall best fit is strongly suggested by figure 3 which shows the diameters required via λ and η to yield the experimental results for argon. The σ_η clearly dominates σ_λ over most of the saturation line, except for the critical region where σ_λ rises sharply in response to a large anomalous increase in thermal conductivity.

Another L-J set that was studied for argon is the pair (120K, 3.4 Å) which gave good results in a study by Rahman[37] of the velocity autocorrelation function. This set yields a closer fit for $\lambda^{MC/RS}$ and η^{WCA} than shown in figures 1 and 2; however, the difference would not be apparent on the figure.

To emphasize the sensitivity to values of L-J parameters, we display in figures 4 and 5 a comparison between theory and experiment for xenon for different sets of L-J properties. The impact of a change in L-J parameters is similar for λ, η_E, η. It is σ_{LJ} which has the greater influence on the transport coefficients. For example, the set (230.05K, 3.95 Å) produces an η^{WCA} that is indistinguishable from the same quantity at (225K, 3.95 Å), shown in figure 5. The L-J parameter values used for these figures are within the range of values used in correlating equilibrium properties, but were chosen to reflect better fits. The best combination here is $\lambda^{MC/RS}$ and η^{WCA}, but this result does not confirm this pair as the overall best combination. These results do seem to show that, for the simplest liquids, best fit to thermal conductivity and shear viscosity can provide a stringent test for choice of MC/RS, WCA, or BH optimization procedures and also for L-J parameters.

Now we may inquire what changes arise when the liquid is not of the simplest kind. A comparison for oxygen is shown in figures 6 and 7. In contrast to the previous results, we find for the set (117.5, 3.386 Å), within the range given to equilibrium correlations, a good fit by $\lambda^{MC/RS}$ and $\eta^{MC/RS}$ and for (117.5K, 3.3 Å), whose σ_{LJ} is outside that range, the indication that for slightly larger σ_{LJ} a good fit is to be had by the WCA or BH route. We can conclude, however, that MD corrections appear necessary, in any case.

A comparison between KRT, MET and experimental values for argon is given in table 1. Herein, KRT thermal conductivity is given by $\lambda^{MC/RS}$ and shear viscosity by η^{WCA}, for the reasons outlined above. The alternate L-J set discussed earlier is used. The MET shear viscosities in the table do not contain MD corrections, as do the MFKT values. This omission may cause one to conclude that better agreement could be had by the MET if MD corrections were included. In the results of ref. 10a, however, it is seen that the MET predictions for the shear viscosity of oxygen are much above the experimental values. Therefore appendage of MD corrections would result in very great disparity between MET predictions and experiment, especially far from the critical point. On the other hand, as we have already shown, the transition from KVT to KRT actually improves the shear viscosity predictions.

In closing this section, we point out that a generalized Eucken relation, derived by Mo and Starling,[38] between thermal conductivity and shear viscosity has the form, for the simplest liquids,

Table 1. Comparison of theoretical and experimental values for thermal conductivity and shear viscosity of saturated liquid argon.

Temp.	Thermal conductivity[a]			Shear viscosity[b]		
T(K)	$\lambda_c^{EXPT.}$	$\lambda_d^{MC/RS}$	λ_e^{MET}	$\eta_c^{EXPT.}$	η_d^{WCA}	η_e^{MET}
85.0	132.2	138.9	---	0.2778	0.3092	---
90.52	122.7	129.5	163.2	0.2364	0.251	0.182
105.6	101.0	105.8	117.6	0.1590	0.1705	0.138
120.7	82.8	84.2	86.6	0.1095	0.121	0.110
135.0	65.7	63.9	---	0.0752	0.084	---
150.0	54.4	35.6	---	0.037	0.042	---

a units are mw/M-K

b units are cp

c from ref. 30

d L-J parameters $\sigma/k = 120K$, $\sigma_{LJ} = 3.4$ Å

e from ref. 10a

$$\lambda = R\left(\frac{15}{4}\,\eta_k\left(1 - \frac{1}{2}\,\frac{\Delta H}{kT}\right) + \frac{5}{2}\,\eta_\phi\right). \qquad (31)$$

Here R is the gas constant and η_k, η_ϕ are the streaming and collisional parts of the shear viscosity. The presence of ΔH, enthalpy departure from the ideal state value, suggests that λ should be sensitive to the whole potential, and more so than the shear viscosity. This could explain the seeming preference for the MC/RS route by thermal conductivity, at least for argon and xenon.

(B) Comparison of Theory and MD Simulation

As a last application, theory and MD simulation for the full L-J potential are compared in table 2. The values ε/k = 119.8 K and σ_{LJ} = 3.405 Å are used (i.e. simulation is made for argon). Two distinct MD approaches are accessible for comparison: the time-correlation function method[39] and nonequilibrium state simulation.[40] Also shown in the table are predictions of the state-dependent-diameter approach using the formulae of KV theory (no hard-sphere MD corrections imposed on shear viscosity) and of KR theory (which includes the hard-sphere MD corrections on shear viscosity[21,22]).

In a broad sense, theory yields remarkable agreement with the MD results. However, the relationship between theory and MD simulation is not made clearcut by this comparison. Hence, despite the specific quantitative successes, expanded upon below, some caution must be exercised in establishing a perspective. First of all, disagreement between predictions of the two MD approaches (cf. point 1) bespeaks the need for further work in this area to develop a set of results which

present a more consistent basis for comparison. Discrepancies between results of 25% are probably not sufficient to clearly signal superiority of one approach over another, at this stage of development in simulation accuracy.

Point 1 shows a comparison between the MD approaches for the same point. Though the results of ref. 39a have been criticized in refs. 40, Ashurst and Hoover have discussed at length[40a,c] the difficulties of simulation near the triple point, represented by point 1, and these presumably carry over to point 5. Note that η^{KR} depends upon time-correlation-function simulation[21] and not nonequilibrium-state simulation, so that our theory here is expected to be more consistent with results of the former type whenever there is discrepancy between results of the two simulation types. (In ref. 40d a shear viscosity result near the triple point obtained via a new nonequlibrium MD approach corroborates the findings attributed to ref. 40a at point 1. Furthermore, in 40d is reported a bulk viscosity of 0.14 cp.) Though inconclusive from a quantitative viewpoint, this comparison shows that the MC/RS diameter is the best choice for thermal conductivity prediction, and, in spite of disagreement with MD results, the KR/WCA and KR/BH ratios for κ/η are compatible with experimental results.[41]

Points 2-4 show a closest overall agreement given by the KR/MC/RS values, in contrast to the findings of the experiment-theory comparison. These results from ref. 39b have been criticized in 39a as being about 30% too small. We offer here further argument to support this assertion. First we note that the MD results are almost uniformly smaller than the KR/WCA shear viscosities by 20%. Like Levesque et al., Gosling et al. compare their MD results to predictions based upon an equivalent hard-sphere model

such that the diameter is chosen to match first peaks between the L-J and equivalent hard-sphere fluid structure factors. The former find a value for this ratio of 0.85, whereas the latter group finds 0.82, 0.83, and 0.83 for the three points 2, 3, 4. Using the numbers and equations supplied by Levesque et al.[39a] we compute a ratio of 1.16 for their point, i.e. it appears an error has been made in their computation for the equivalent hard-sphere shear viscosity. If this ratio is a reliable measure(which underscores the theme of this section) then we conclude that Gosling's et al. results are systematically low, by an amount that would bring them into close agreement with the KR/WCA values.

Points 6-9 fall on or near the saturation curve which underlies the experimental results shown in figure 2, though the shear viscosities themselves do not fall on that experimental line. Herein we obtain extremely close agreement to MD results with MFK/WCA theory, over a significant portion (101.8 - 147.1 K, at least) of the saturation curve. Clearly, here the WCA diameter represents the best choice for shear viscosity prediction. Of course, this result may not carry over to the comparison with experiment, since there, the simple theory we are using must absorb a number of real-system features which are not built into our L-J model. Finally we note the overall quantitative superiority of the KR/WCA theory for shear viscosity compared to the MET when applied to the simulation at points 5, 6, 7, 8.[40a]

Table 2. Comparison of theoretical and MD values for shear (η) and bulk (κ) viscosities (in cp) and thermal conductivity (λ, in mw/M-K) for the L-J fluid, with ε/k = 119.8 K, σ_{LJ} = 3.405 Å. MD results from ref. 39 are for Green-Kubo expressions, those from ref. 40 for nonequilibrium MD simulation

			Theory			MD
			MC/RS	WCA	BH	
1.	ρ = 1.418 gm/cc	η	0.224 (KR)	0.210 (KV)	0.217 (KV)	0.364 (Ref. 39a) [0.348*]
	T = 86.5 K			0.342 (KR)	0.377 (KR)	0.262 ± 0.009 (Ref. 40a)
		λ	143.9	172.0	177.6	124.1 ± 7.5 (Ref. 40a)
		κ	0.20	0.247	0.257	0.095 (Ref. 39a)
		κ/η	0.89 (KR)	0.72 (KR)	0.68 (KR)	0.26 (Ref. 39a)
2.	ρ = 1.346 gm/cc	η	0.174 (KR)	0.182 (KV)	0.187 (KV)	0.183 (Ref. 39b)
	T = 112.3 K			0.226 (KR)		
3.	ρ = 1.228 gm/cc	η	0.126 (KR)	0.137 (KV)	0.139 (KV)	0.128 (Ref. 39b)
	T = 120.4 K			0.153 (KR)		
4.	ρ = 1.051 gm/cc	η	0.083 (KR)	0.092 (KV)	0.092 (KV)	0.077 (Ref. 39b)
	T = 139.3 K			0.095 (KR)		
5.	ρ = 1.4327 gm/cc	η	0.239 (KR)	0.218 (KV)	0.225 (KV)	0.297 (Ref. 40a)
	T = 83.9 K			0.385 (KR)		
6	ρ = 1.2777 gm/cc	η	0.1431 (KR)	0.1765 (KR)	0.1815 (KR)	0.1734 (Ref. 40a)
	T = 104.5 K					
7.	ρ = 1.1621 gm/cc	η	0.1060 (KR)	0.1249 (KR)	0.1268 (KR)	0.1255 (Ref. 40a)
	T = 119.56 K					

Table 2, continued

8.	$\rho = 0.8017$ gm/cc $T = 147.1$ K	η	0.0497 (KR)	0.0536 (KR)	0.0536 (KR)	0.0579 (Ref. 40a)
9.	$\rho = 1.2763$ gm/cc $T = 101.83$ K	η	0.142 (KR)	0.149 (KV) 0.175 (KR)	0.152 (KV) 0.180 (KR)	0.172 ± 0.005 (Ref. 40b)

*Unpublished result by Levesque, shown in ref. 40d.

VI. DISCUSSION

For a hard-core potential both KVT and KRT engender the association (20) which is a primary element in the MET method[10a] for applying the Enskog theory transport coefficients[7a] to real substances. For soft-core potentials, however, both KVT and KRT support a more general route in relating hard-sphere transport coefficients to those of real substances, which utilizes a consistent interpretation of the quantities σ and y_2 as hard-sphere quantities described in terms of a state-dependent diameter chosen for representation of thermodynamics that is optimal in one of several well-defined senses. In the applications investigated so far, on saturated simple liquids, this use of a state-dependent diameter on a fundamentally consistent level is quantitatively superior to the MET, and appears to be conceptually cleaner and technically more tractable than the MET. In addition, the mixture versions of KVT[42] and KRT lead to a natural generalization of our methods,[43] whereas, for the MET, no mixture analog of (20) exists.

Our numerical results already demonstrate a good agreement between theory and experiment, via the Lennard-Jones model and for L-J parameters appropriate to description of equilibrium phenomena. Even though our theory is purely "classical" in its description of the critical region, providing no allowance for anomalous critical behavior, it yields good results even into the critical region where the thermal conductivity is known to exhibit a large anomalous increase and the shear viscosity behavior is more regular.[44] For thermal conductivity, in particular, the results we obtain here are best regarded as describing the background terms against which the critical anomalous increases are measured. We note some related earlier work. For liquids, Ely and McQuarrie[45] used a BH/MET combination whose accuracy is surpassed by our KRT/WCA approach. Complementary to

our work is that of Dymond and Alder[46] who defined a temperature-dependent diameter by fit of (19) to experimental gas pressures and thence obtained good predictions for dense gas transport properties. We have begun a study to determine the best combinations for diameter assignment, among the MC/RS, BH and WCA approaches, and the best L-J parameter set for overall best fit of theory to experiment. Results will be reported at a later date. Failure of the MET to accurately predict results obtained by molecular dynamics[47] is not surprising in the light of our work here, which suggests that it would be of great interest to apply our state-dependent-diameter approach to the soft-sphere system studied by Hoover.[47b]

In summary, the kinetic variational theory is conceptually robust from several viewpoints. It plays a central role as a general kinetic theory in relation to previously known theories. It furnishes a theoretical basis for the MET. It interfaces cleanly with the already established program of optimized thermodynamic approximation, whereby interpretation of all variables in the transport-coefficient formulae is made naturally in hard-sphere terms. The kinetic variational theory also contains an entropy functional, and the kinetic equation gives rise to an H-theorem. The KVT shear viscosity and self-diffusion coefficients admittedly suffer the inaccuracies incumbent upon the velocity chaos assumption; we have shown how these can be removed by generalizing the theory. The resulting KRT shares all the desirable predictive properties of the KVT above, although we can no longer identify an entropy functional and prove an H-theorem.

The alteration of the KV shear viscosity that is manifested by the KRT is such as to improve the agreement between theory and experiment and theory and MD simulation, especially when the formulae are interpreted in the framework of the state-dependent-diameter approach. Under these conditions, our results suggest that in comparison with MD simulation on simple liquids, the MC/RS and WCA diameters are most appropriate to correlate thermal conductivity and shear viscosity, respectively. In comparison with experiment, this is not as clear, but the same correlation is strongly suggested by our preliminary investigation.

The KV and KR theories we have introduced here are but two members of a family of kinetic "weighted mean-field" theories defined by Eq. (2). Both use the equilibrium pair distribution function g_2^{HS} of a hard-sphere system as the weight function G in the mean-field term of (2) and differ only in the choice of the weight function in the collision term. One can also contemplate using the full equilibrium pair distribution function g_2 instead of the hard-sphere reference-system g_2^{HS} in either the mean-field or collision term; we hope to explore the results of this and other choices as well as the rationale for the kinetic equations they yield. A systematic study in this framework is yet to be made and appears worthwhile.[48]

ACKNOWLEDGMENTS

The authors wish to acknowledge the support of this work by the Office of Basic Energy Sciences, U.S. Department of Energy. John Karkheck is also indebted to the National Science Foundation for his support while pursuing this research. Finally we wish to acknowledge discussions with Dr. John Kincaid in regard to the MET and mixtures.

REFERENCES

1. J. G. Kirkwood et al. J. Chem. Phys. 14, 180 (1946); 17, 988 (1949); 21, 2050 (1953); 31, 901 (1959).

2. M. Born and H. S. Green, A General Kinetic Theory of Liquids (Cambridge Univ. Press, 1949).

3. S. A. Rice and A. R. Allnatt, J. Chem. Phys. 34, 2144, 2156 (1961).

4. H. T. Davis, S. A. Rice and J. V. Sengers, J. Chem. Phys. 35, 2210 (1961).

5. See, for example, R. Zwanzig, Ann. Rev. Phys. Chem. 16, 67 (1965).

6. Boltzmann's kinetic theory is the prototype. See L. Boltzmann, Lectures on Gas Theory (Univ. of California Press, Berkeley, 1964).

7a. D. Enskog, K. Sven. Vetenskapsakad. Handl. 63(4) (1922), a translation of which appears in S. G. Brush, Kinetic Theory V. 3 (Pergamon Press, Oxford, 1972). See also S. Chapman and T. G. Cowling, The Mathematical Theory of Nonuniform Gases, Cambridge Univ. Press, 1970. 7b. We note for clarity our terminology: the standard Enskog theory (SET) refers to the kinetic equation and transport coefficient formulae found in ref. 7a. The RET kinetic equation differs from that of SET, but for a one-component fluid the transport coefficient formulae are the same. The MET, though occasionally confused in the literature with the SET, is no more than a methodological prescription for interpreting these formulae in real fluid terms.

8. H. van Beijeren and M. H. Ernst, Physica 68, 437 (1973); 70, 225 (1973).

9. P. Resibois, Phys. Rev. Lett. 40, 1409 (1978); J. Stat. Phys. 19, 593 (1978).

10. a. H. J. M. Hanley, R. D. McCarty and E. G. D. Cohen, Physica 60, 322 (1972).

b. H. J. M. Hanley, Cryogenics 16, 643 (1976).

c. R. DiPippo et al., Physica 86A, 205 (1977).

11. a. H. H. Thorne, in S. Chapman and T. G. Cowling, op. cit.

11. b. M. K. Tham and K. E. Gubbins, J. Chem. Phys. 55, 268 (1971).

c. J. M. Kincaid, Phys. Lett. 64A, 429 (1978).

d. J. Karkheck and G. Stell, J. Chem. Phys. 71, 3636 (1979).

12. For consistency in representation into the dilute gas regime, the diameter cannot be chosen arbitrarily. See ref. 28a.

13. J. Karkheck and G. Stell, Bull. Am. Phys. Soc. 25, 349 (1980) and SUNY CEAS Report #334, December, 1979.

14. M. Grmela, J. Math. Phys. 15, 35 (1974).

15. M. Kac, P. C. Hemmer and G. E. Uhlenbeck, J. Math. Phys. 4, 216, 229 (1963); 5, 60 (1964).

16. J. Percus and G. J. Yevick, Phys. Rev. 136B, 290 (1964).

17. a. J. D. Weeks, D. Chandler and H. C. Andersen, J. Chem. Phys. 54, 5237 (1971).

b. L. Verlet and J. J. Weis, Phys. Rev. A 5, 939 (1972); Mol. Phys. 24, 1013 (1972).

18. G. A. Mansoori and F. B. Canfield, J. Chem. Phys. 51, 4958 (1969).

19. J. Rasaiah and G. Stell, Mol. Phys. 18, 249 (1970).

20. J. A. Barker and D. Henderson, J. Chem. Phys. 47, 4714 (1967).

21. B. J. Alder, D. M. Gass and T. E. Wainwright, J. Chem. Phys. 53, 3813 (1970).

22. J. H. Dymond, Physica 85A, 175 (1976).

23. This also follows straightforwardly by substituting $f_2 = g_2^{HS} f_1 f_1$ into eq. 6.24 of J. H. Irving and J. G. Kirkwood, J. Chem. Phys. 18, 817 (1950).

24. J. T. O'Toole and J. S. Dahler, J. Chem. Phys. 32, 1097 (1960).

25. S. Chapman and T. G. Cowling, op cit., Ch. 7.

26. J. A. Barker and D. Henderson, Rev. Mod. Phys. 48, 587 (1976).

27. A. Isihara, J. Phys. A 1, 539 (1968).

28. a. J. Hirschfelder, C. F. Curtiss, and R. B. Bird, Molecular Theory of Gases and Liquids, John Wiley and Sons, New York, 1954.

b. A. Michels and R. O. Gibson, Proc. R. Soc. A 134, 288 (1931).

29. a. M. Napiorkowski, J. Piasecki, M. Seghers, and P. Resibois, J. Chem. Phys. 66, 1422 (1977).

b. P. Resibois, J. Piasecki, and Y. Pomeau, Phys. Rev. Lett. 28, 882 (1972).

30. H. J. M. Hanley, R. D. McCarty, and W. M. Haynes, J. Phys. Chem. Ref. Data 3, 998 (1974).

31. E. Helfand and S. A. Rice, J. Chem. Phys. 32, 1642 (1960).

32. M. K. Tham and K. E. Gubbins, I & EC Fundamentals 8, 791 (1969).

33. M. K. Tham and K. E. Gubbins, I & EC Fundamentals 9, 63 (1970).

34. N. F. Carnahan and K. E. Starling, J. Chem. Phys. 53, 600 (1970).

35. B. Larsen, J. C. Rasaiah, and G. Stell, Mol. Phys. 33, 987 (1977).

36. T. M. Reed and K. E. Gubbins, Applied Statistical Mechanics, McGraw-Hill, Inc., New York, 1973, pp. 410-411.

37. A. Rahman, Phys. Rev. 136A, 405 (1964).

38. K. C. Mo and K. E. Starling, in Applications of Multiparameter Corresponding States Theory for Prediction of Polar, Polyatomic Fluid Transport Properties, NSF/ENG77-21511 Report, U. of Oklahoma.

39. a. D. Levesque, L. Verlet, and J. Kürkijarvi, Phys. Rev. A 7, 1690 (1973).

b. E. M. Gosling, I. R. McDonald, and K. Singer, Mol. Phys. 26, 1475 (1973).

40. a. W. T. Ashurst and W. G. Hoover, Phys. Rev. A 11, 658 (1975).

b. D. J. Evans, J. Stat. Phys. 22, 81 (1980).

c. W. T. Ashurst and W. G. Hoover, Phys. Lett. 61A, 175 (1977).

d. W. G. Hoover, D. J. Evans, R. B. Hickman, A. J. C. Ladd, W. T. Ashurst, B. Moran, Phys. Rev. A 22, 1690 (1980).

41. J. A. Cowan and R. N. Ball, Can. J. Phys. 50, 1881 (1972).

42. J. Karkheck, G. Stell and E. Martina, to be published.

43. Generalizations to mixtures of the MC/RS, WCA, and BH procedures have been developed: see G. A. Mansoori and T. W. Leland, Jr., J. Chem. Phys. 53, 1931 (1970), L. L. Lee and D. Levesque, Mol. Phys. 26, 1351 (1973), and E. W. Grundke, D. Henderson, J. A. Barker and P. J. Leonard, Mol. Phys. 25, 883 (1973), respectively.

44. J. V. Sengers, in Transport Phenomena-1973, J. Kestin ed., A.I.P. Conference Proceedings No. 11 (AIP, New York, 1973).

45. J. F. Ely and D. A. McQuarrie, J. Chem. Phys. 60, 4105 (1974).

46. J. H. Dymond and B. J. Alder, J. Chem. Phys. 45, 2061 (1966).

47. a. J. P. J. Michels and N. J. Trappeniers, Physica 101A, 156 (1980).

b. W. G. Hoover, A. J. C. Ladd, R. B. Hickman and B. L. Holian, Phys. Rev. A 21, 1756 (1980).

48. An interesting related study with somewhat different viewpoint and emphasis has been made by M. Grmela and L. S. Garcia-Colin, Phys. Rev. A 22, 1295, 1305 (1980).

FIGURE CAPTIONS

Figure 1. Comparison of theoretical and experimental thermal conductivities for saturated liquid argon. The MC/RS (refs. 18, 19), WCA (ref. 17), and BH (ref. 20) curves reflect state-dependent diameters based upon the L-J parameters ε/k = 119.8 K, σ_{LJ} = 3.405 Å. The DRS result for the square-well potential was taken from ref. 36.

Figure 2. Comparison of theoretical and experimental shear viscosities for saturated liquid argon. Results without and with MD correction factors are shown. The L-J parameters ε/k = 119.8 K, σ_{LJ} = 3.405 Å underlie the state-dependent diameters found via the MC/RS, WCA and BH procedures. The DRS result, from ref. 36, does not contain MD corrections beyond the basic DRS formula (ref. 4).

Figure 3. Effective diameters σ_λ and σ_η to reproduce experimental thermal conductivity and shear viscosity of saturated liquid argon via (27a) and (27b) with MD corrections, respectively.

Figure 4. Comparison of theoretical and experimental thermal conductivities for saturated liquid xenon. The L-J sets (225 K, 4.05 Å) and (225 K, 3.95 Å) underlie, respectively, the subscript 1 curves and subscript 2 curves.

Figure 5. Comparison of theoretical and experimental shear viscosities for saturated liquid xenon. Results without and with MD correction factors are shown. The L-J set (225 K, 4.05 Å) relates to subscript 1 curves and the set (225 K, 3.95 Å) to subscript 2 curves.

Figure 6. Comparison of theoretical and experimental thermal conductivities for saturated liquid oxygen. The subscript 1 curves are based upon the L-J set (117.5 K, 3.386 Å), and the subscript 2 curves upon the set (117.5 K, 3.3 Å).

Figure 7. Comparison of theoretical and experimental shear viscosities for saturated liquid oxygen. The L-J set (117.5 K, 3.386 Å) relates to subscript 1 curves and the set (117.5 K, 3.3 Å) to subscript 2 curves.

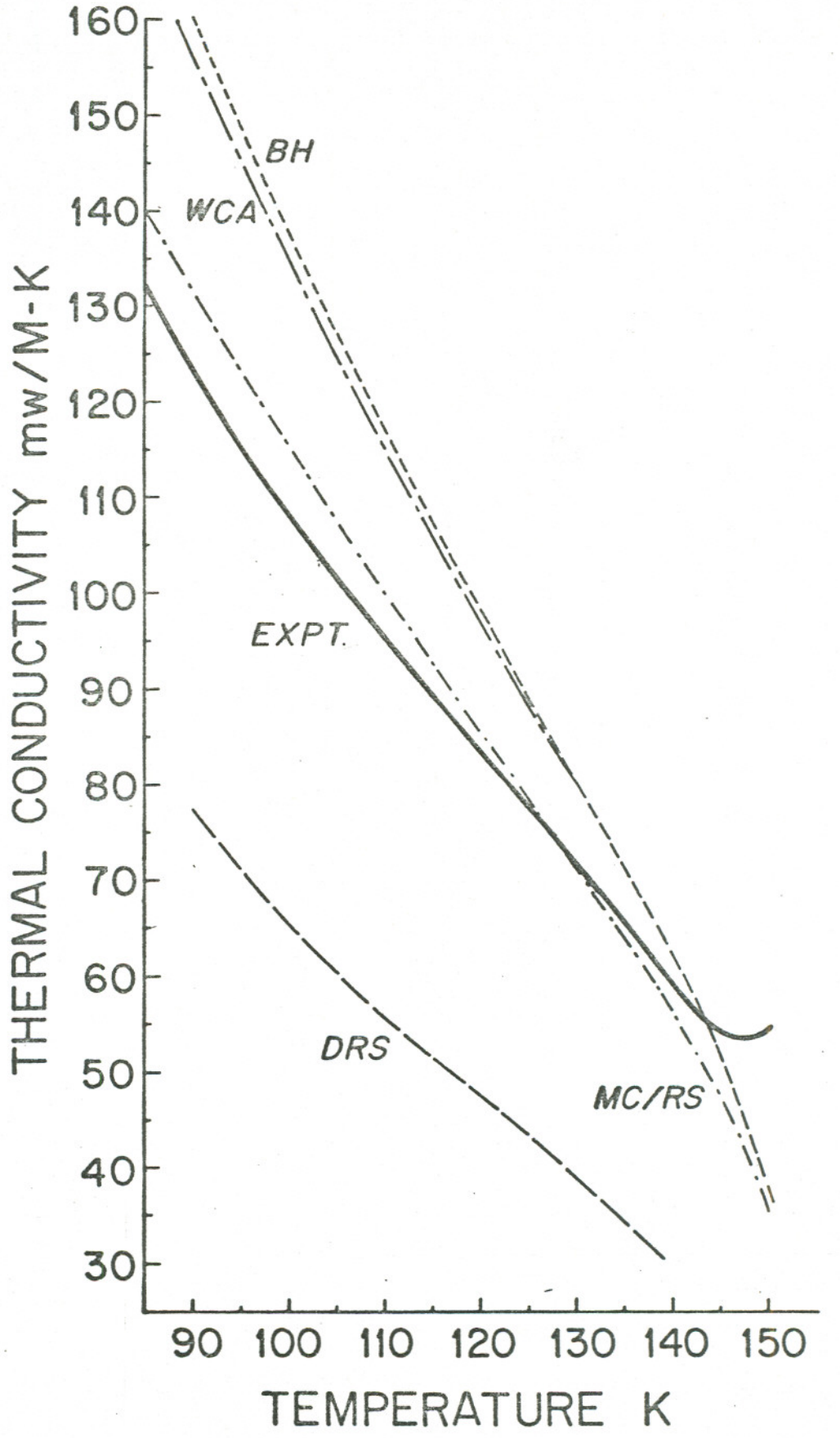
160
150
140
130
120
110
100
90
80
70
60
50
40
30
THERMAL CONDUCTIVITY mw/M-K
BH
WCA
EXPT.
DRS
MC/RS
90 100 110 120 130 140 150
TEMPERATURE K

Fig. 1

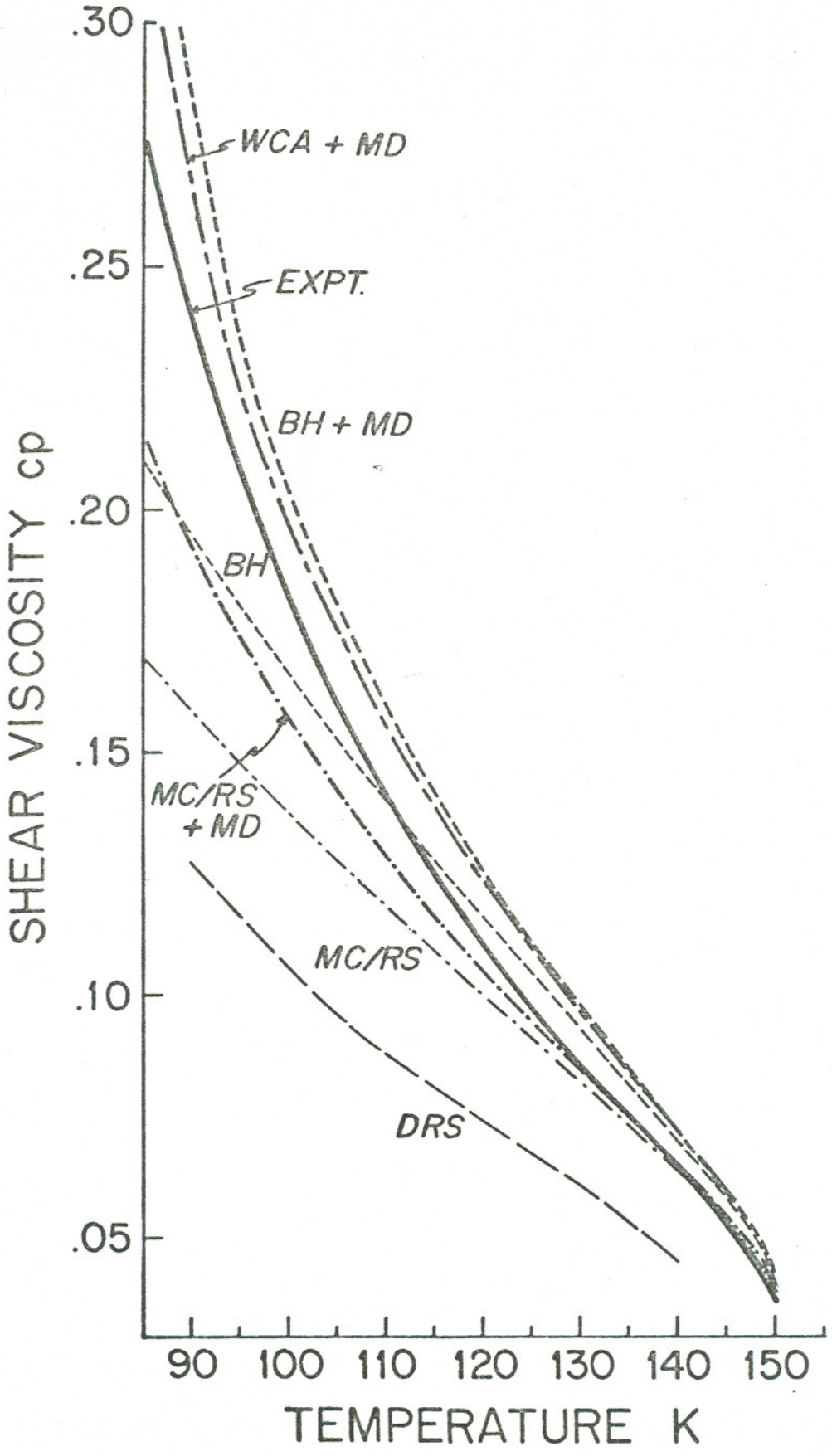
.30
.25
.20
.15
.10
.05
SHEAR VISCOSITY cp
WCA + MD
EXPT.
BH + MD
BH
MC/RS
+ MD
MC/RS
DRS
90
100
110
120
130
140
150
TEMPERATURE K

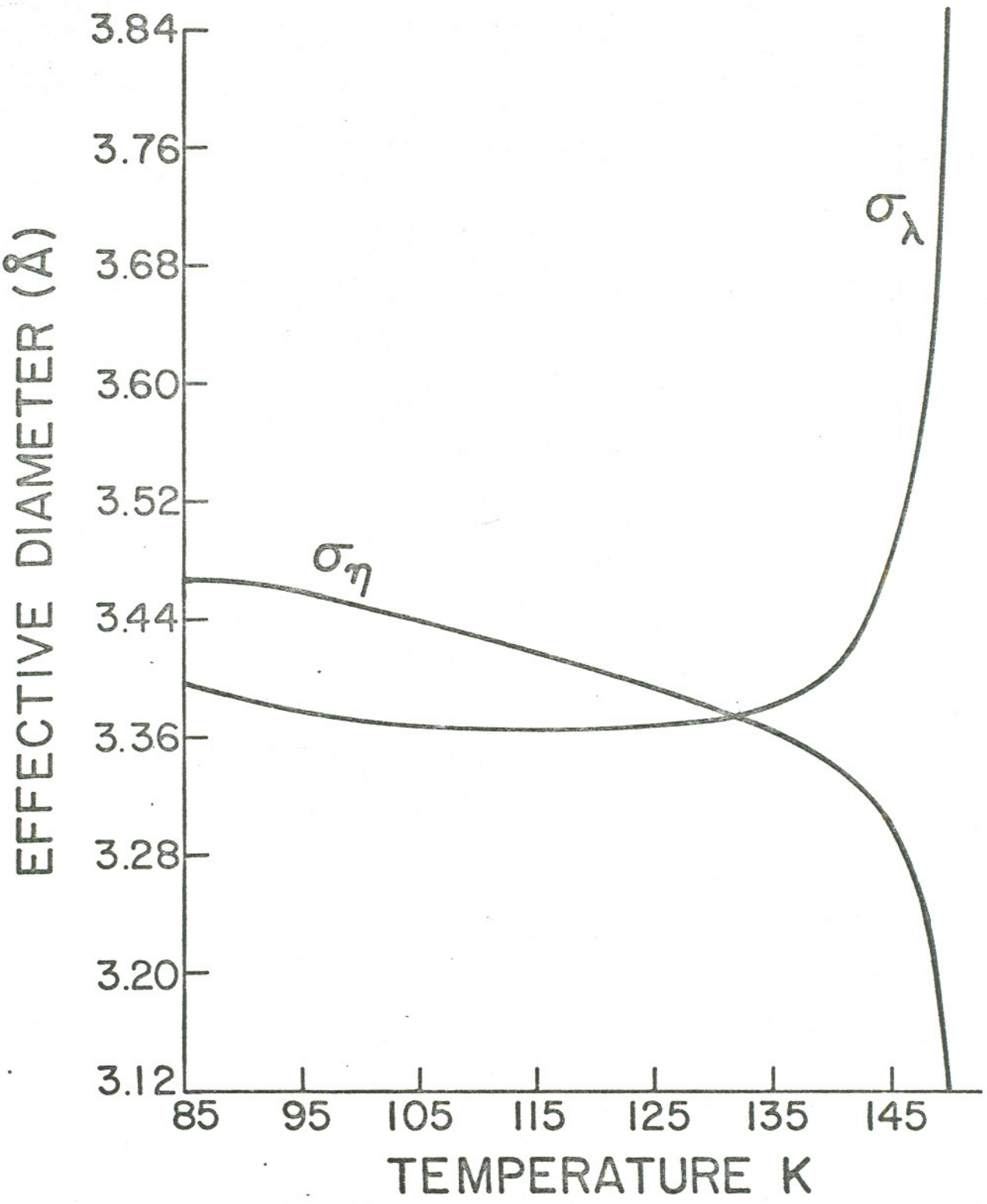
3.84
3.76
3.68
3.60
3.52
3.44
3.36
3.28
3.20
3.12
EFFECTIVE DIAMETER (Å)
σ_λ
σ_η
85
95
105
115
125
135
145
TEMPERATURE K

Fig.3

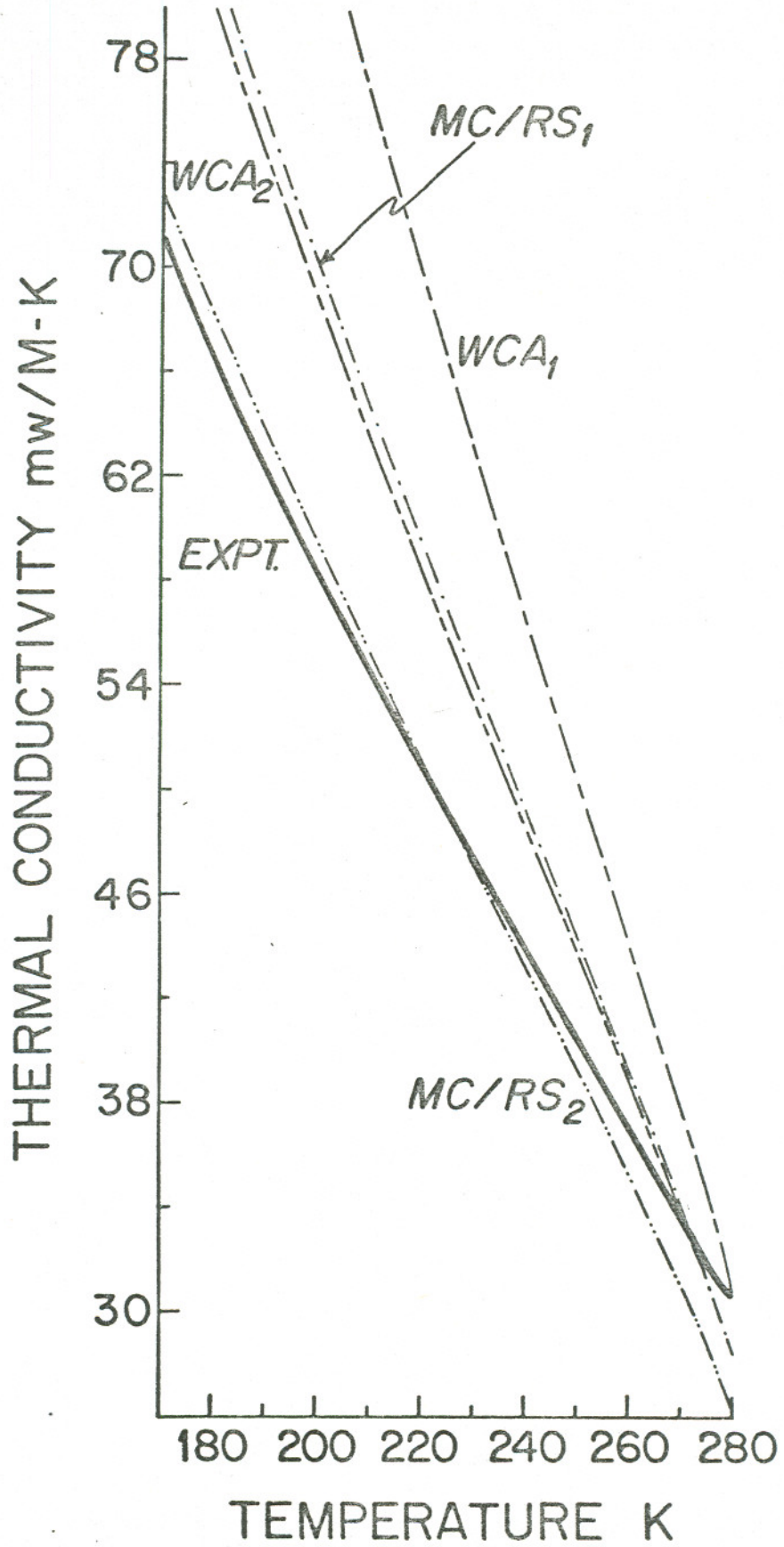
78
70
62
54
46
38
30
THERMAL CONDUCTIVITY mw/M-K
MC/RS1
WCA2
WCA1
EXPT.
MC/RS2
180 200 220 240 260 280
TEMPERATURE K

Fig. 4

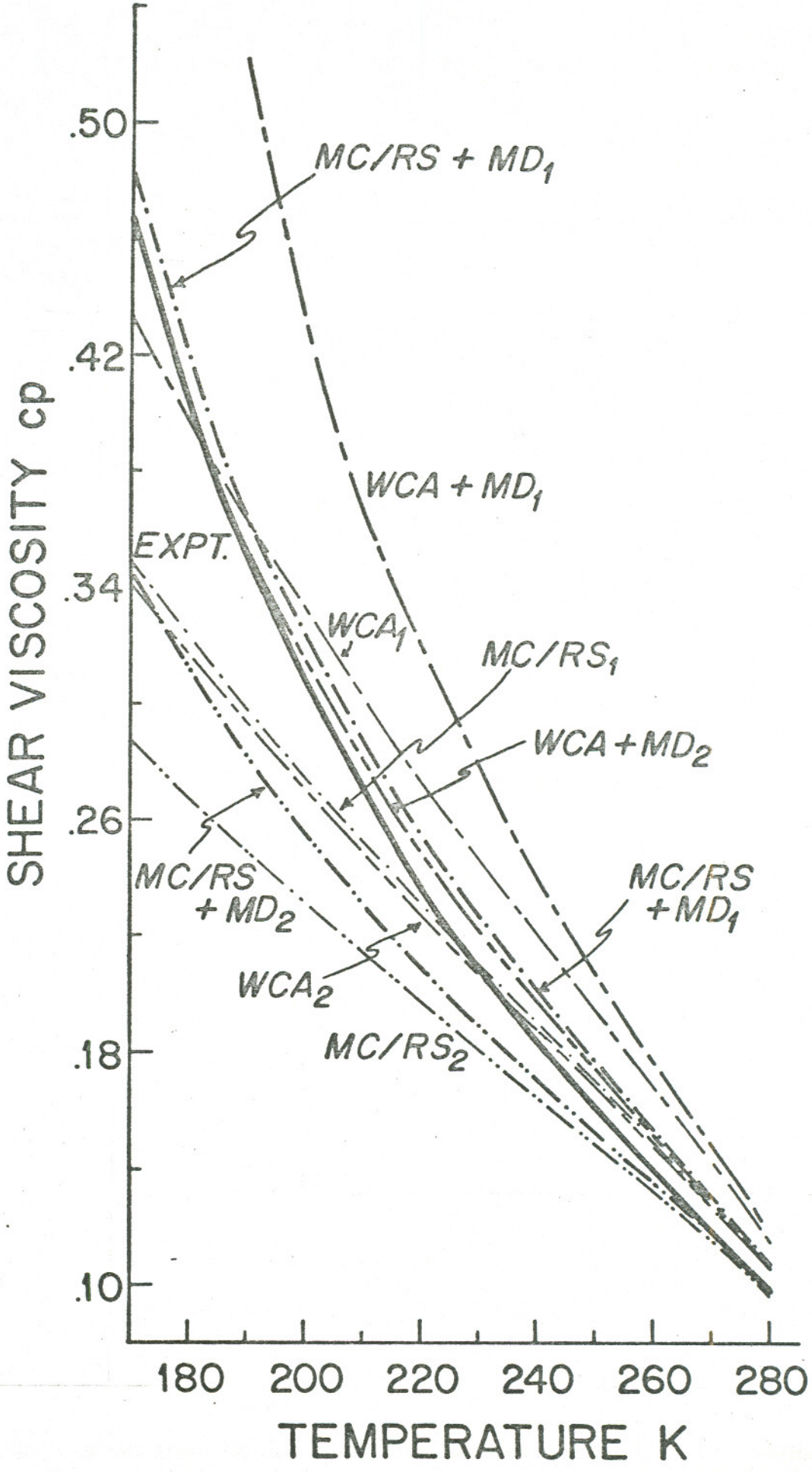
SHEAR VISCOSITY cp
.50
.42
.34
.26
.18
.10
180
200
220
240
260
280
TEMPERATURE K
MC/RS + MD1
WCA + MD1
EXPT.
WCA1
MC/RS1
WCA + MD2
MC/RS + MD2
MC/RS + MD1
WCA2
MC/RS2

Fig. 5

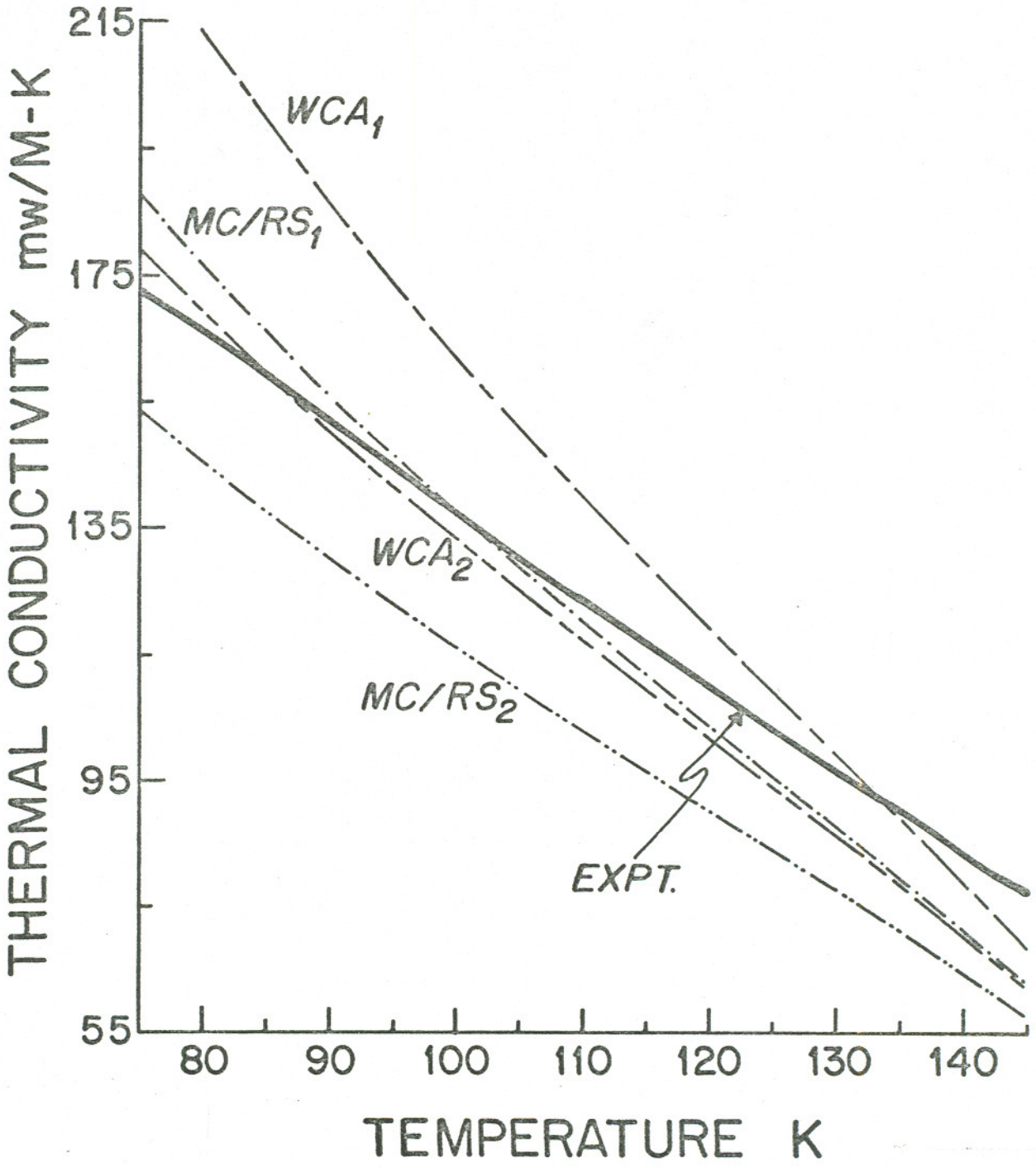
THERMAL CONDUCTIVITY mw/M-K
215
175
135
95
55
80
90
100
110
120
130
140
TEMPERATURE K
WCA1
MC/RS1
WCA2
MC/RS2
EXPT.

Fig. 6

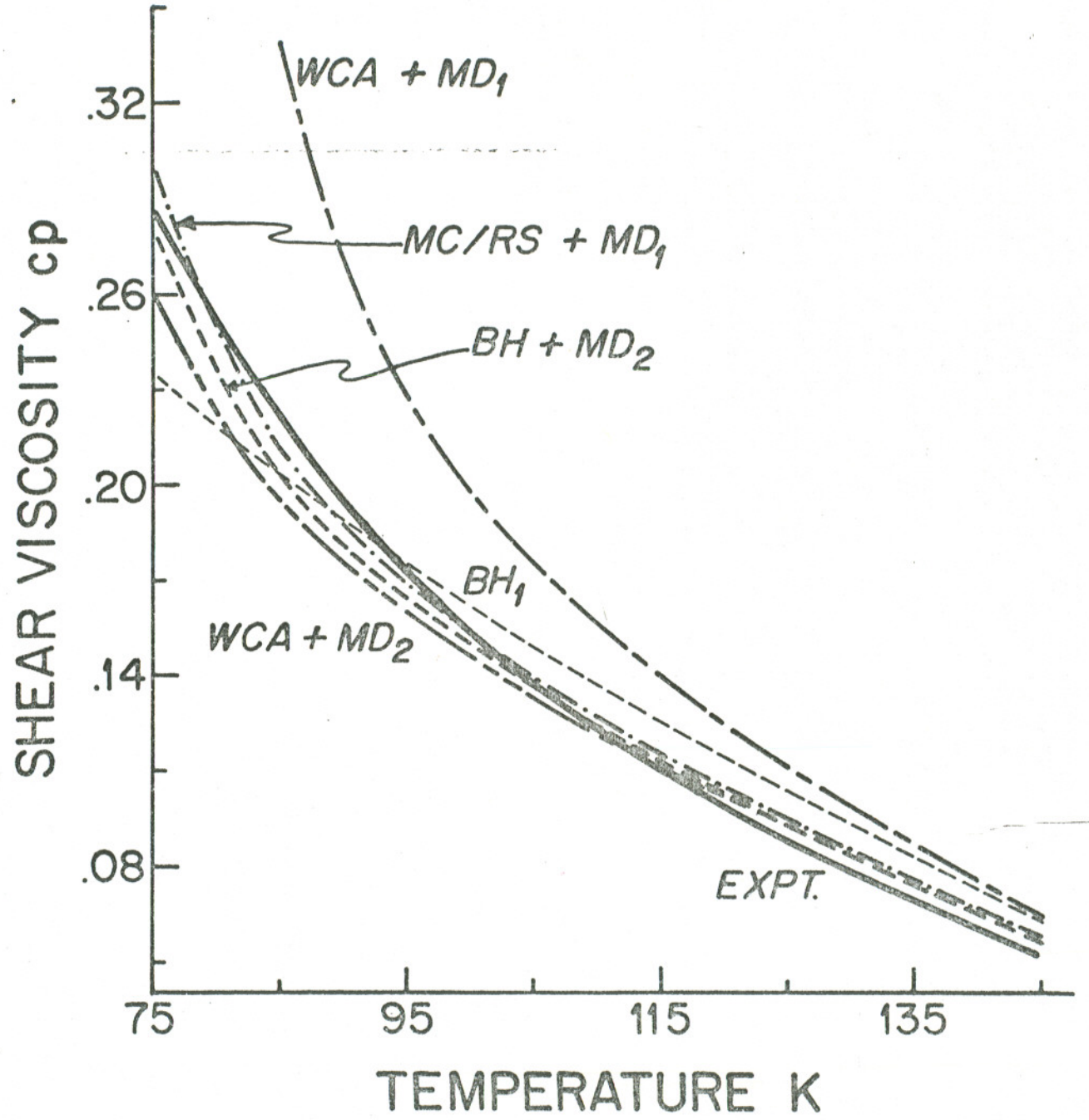
WCA + MD1
MC/RS + MD1
BH + MD2
BH1
WCA + MD2
EXPT.
SHEAR VISCOSITY cp
.32
.26
.20
.14
.08
75
95
115
135
TEMPERATURE K